Predictive Three-Dimensional Quantitative Structure−Activity Relationship of Cytochrome P450 1A2 Inhibitors

Laura E. Korhonen,*,† Minna Rahnasto,† Niina J. Mähönen,† Carsten Wittekindt,‡ Antti Poso,‡ Risto O. Juvonen,† and Hannu Raunio†

Department of Pharmacology and Toxicology and Department of Pharmaceutical Chemistry, University of Kuopio, POB 1627, 70211 Kuopio, Finland

Received December 21, 2004

The purpose of this study was to determine the cytochrome P450 1A2 (CYP1A2) inhibition potencies of structurally diverse compounds to create a comprehensive three-dimensional quantitative structure−activity relationship (3D-QSAR) model of CYP1A2 inhibitors and to use this model to predict the inhibition potencies of an external set of compounds. Fifty-two compounds including naphthalene, lactone and quinoline derivatives were assayed in a 96-well plate format for CYP1A2 inhibition activity using 7-ethoxyresorufin O-dealkylation as the probe reaction. The IC_{50} values of the tested compounds varied from 2.3 μM to over 40 000 μM. On the basis of this data set, a comparative molecular field analysis (CoMFA) and GRID/GOLPE models were created that yielded novel structural information about the interaction between inhibitory molecules and the CYP1A2 active site. The created CoMFA model was able to accurately predict inhibitory potencies of several structurally unrelated compounds, including selective inhibitors of other cytochrome P450 forms.

Introduction

Microsomal cytochrome P450 (CYP) enzymes are a family of heme proteins involved in the metabolism of numerous toxic and pharmacologically active compounds. In humans, the CYP1A2 enzyme is expressed at a high level only in the liver, where it constitutes approximately 10% of the total cytochrome P450 content. It is one of the enzymes responsible for the activation of aromatic and heterocyclic amines and polycyclic aromatic hydrocarbons to reactive metabolites.[1,2] Many pharmaceuticals, e.g., caffeine[3] and theophylline[4] are selective substrates for CYP1A2, and the enzyme is effectively inhibited by furafylline[5] and fluvoxamine.[6,7] A complete list of CYP1A2 substrates and inhibitors is provided at the Web site http://medicine.iupui.edu/flockhart.

Rapid advances in several different technologies have yielded increasingly precise information on the interactions between cytochrome P450 and their ligands. In particular, quantitative structure−activity relationship (QSAR) and pharmacophore approaches have been used to assess the active sites of cytochrome P450. These new computational models are promising tools to screen more rapidly the quantitative interactions between chemicals and cytochrome P450 enzymes. However, these techniques are still in the early stages of development with respect to application for cytochrome P450 and there is plenty of scope for technological improvement.[8]

Several computational approaches, especially QSARs, have been used to characterize the molecular properties of substrates and inhibitors of the CYP1A2 enzyme. The overall result of these studies is that substrates of CYP1A2 are moderately basic and planar molecules with medium volume and low total interaction energies (ΔE value), but there is no clear correlation between compound lipophilicity and inhibitory effect.[9−15]

There are no reports on the use of pharmacophore or QSAR techniques to characterize the molecular properties of CYP1A2 inhibitors and then to use this information for quantitative prediction. Therefore, the goals of this study were to determine the CYP1A2 inhibition potencies of structurally diverse compounds, to create a comprehensive 3D-QSAR model of CYP1A2 inhibitors, and to use this model to predict the inhibition potencies of an external set of compounds. To achieve this goal, the abilities of 52 compounds including naphthalene, lactone, and quinoline derivatives to inhibit CYP1A2-catalyzed 7-ethoxyresorufin O-dealkylation reaction were examined. On the basis of this data set, a comparative molecular field analysis (CoMFA) and a GRID/GOLPE analysis were carried out. The generated CoMFA model yielded precise information about the molecular characteristics of CYP1A2 inhibitors and was able to accurately predict the inhibitory potencies of several structurally unrelated compounds.

Results

Inhibition of CYP1A2 Activity. CYP1A2 substrates and inhibitors are usually planar small-volume molecules that are neutral or weakly basic. Fifty-two naphthalene and lactone derivatives as well as other compounds partially fitting these criteria were tested for inhibitory potency toward the CYP1A2 enzyme. The structures of the compounds are shown in Figures 1 and 2.

The IC_{50} values of these compounds were measured using 7-ethoxyresorufin O-dealkylation as the probe

* To whom correspondence should be addressed. Telephone: +358-17-163778. Fax: +358-17-162424. E-mail: Laura.Korhonen@uku.fi.
† Department of Pharmacology and Toxicology.
‡ Department of Pharmaceutical Chemistry.

10.1021/jm0489713 CCC: $30.25
Published on Web 05/05/2005

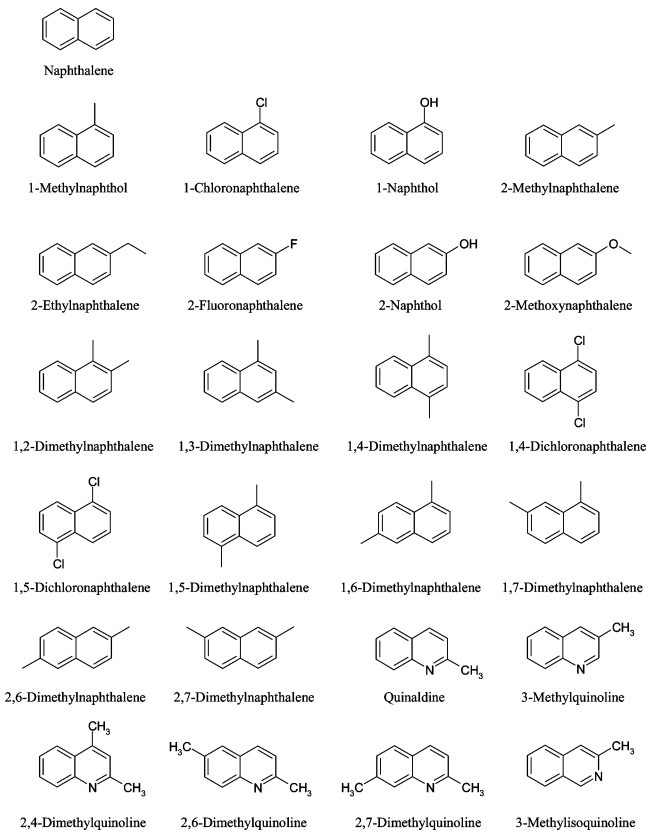

Figure 1. Structures of naphthalene-type compounds used in inhibition assays.

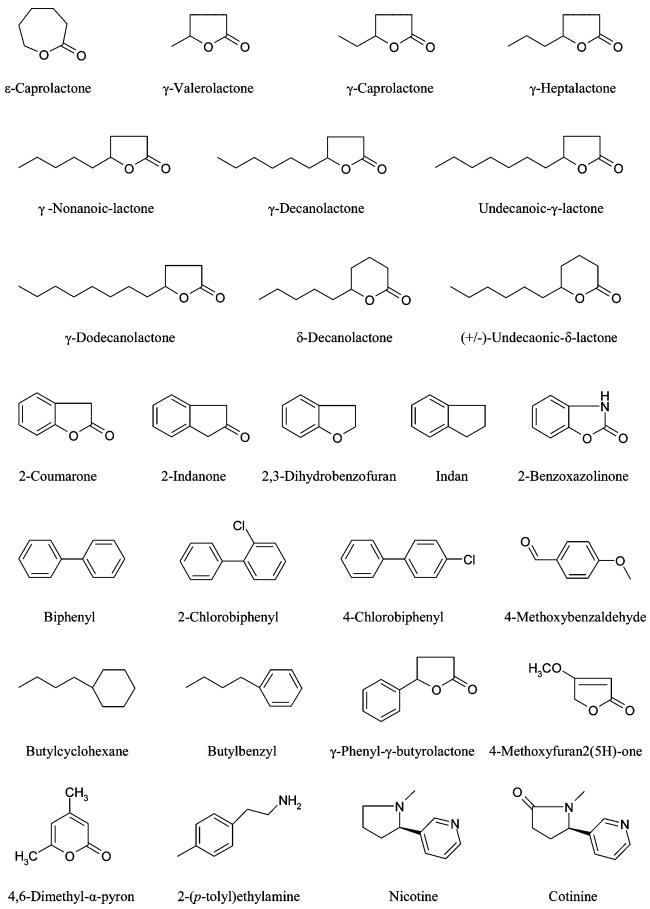

Figure 2. Structures of lactones and other compounds used in inhibition assays.

reaction. Recombinant human CYP1A2 was used as the enzyme source to exclude any interference from other cytochrome P450 forms present in human liver microsomes. The enzymatic activity was assayed under constant conditions using seven different concentrations of each inhibitor. Figure 3 represents an example of concentration-dependent inhibition of the enzyme activity by two structurally different compounds (2,6-dimethylquinoline and 2-methylnaphthalene).

The lowest IC_{50} values were obtained with 1,4-dichloronaphthalene and 2,4-dimethylquinoline (<3 μM), and the highest values were obtained with ϵ-caprolactone and 4-methoxyfuran-2(5*H*)-one (>40 mM) (Tables 1 and 2). Most of the naphthalene derivatives were more potent inhibitors than the lactones and other compounds tested.

The IC_{50} values of all naphthalene derivatives were lower than the IC_{50} value of naphthalene because methyl, chloro, ethyl, fluoro, and hydroxyl substitutions decreased the IC_{50} value. In general, disubstituted naphthalenes or quinolines were more potent than monosubstituted or unsubstituted ones. In particular, electronegative substitutions at position 1 of naphthalene increased the inhibitory potency. The IC_{50} values of quinoline derivatives were lower than the corresponding naphthalene derivatives, indicating that a heterocyclic nitrogen atom decreases the IC_{50} value (Table 1).

The inhibitory potencies of 11 lactones were tested (Table 2). The simple lactone ring structures were weak inhibitors, ϵ-caprolactone being the least potent. With alkyl-substituted γ- and δ-lactones, the inhibition potency increased with increasing side chain length. The optimum length of the side chain was seven carbons. The IC_{50} value decreased more than 300-fold when the side chain length increased from methyl to hexyl in five ring lactones. The most potent lactone inhibitor was undecanoic-γ-lactone (IC_{50} = 45 μM).

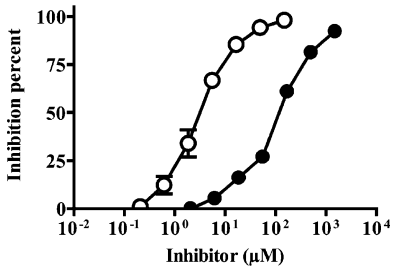

Figure 3. Inhibition of CYP1A2 activity by two selected compounds. 2,6-Dimethylquinoline (○) and 2-methylnaphthalene (●) were used as inhibitors.

In addition to lactone and naphthalene derivatives, other selected compounds were tested for CYP1A2 inhibition (Table 2). When the cyclohexane ring of butylcyclohexane was replaced by phenyl, the IC_{50} value increased about 60-fold. 2-Coumarone and 2-indanone, which have a carbonyl group, were more potent inhibitors than indan and 2,3-dihydrobenzofuran. A halogen group at position 4 of the biphenyl increased inhibitory potency, and that at position 2 decreased inhibitory potency.

CoMFA and GRID/GOLPE Analysis. Forty-six compounds listed in Tables 1 and 2 were analyzed using CoMFA and GRID/GOLPE methods. Also listed in

Table 1. Inhibition Potencies of Naphthalene-Type Compounds for CYP1A2

compd	IC_{50} (μM)	95% confidence intervals	pIC_{50}
1,4-dichloronaphthalene	2.3	0.9−3.7	5.64
2,4-dimethylquinoline	2.4	1.5−3.2	5.62
1-naphthol	3.2	2.4−4.0	5.49
2,6-dimethylquinoline	3.3	2.7−3.9	5.48
1,4-dimethylnaphthalene	3.6	2.8−4.2	5.44
2,7-dimethylquinoline	4.4	3.5−5.3	5.36
1,2-dimethylnaphthalene	5.5	3.4−7.6	5.26
1,7-dimethylnaphthalene	7.5	4.5−11	5.12
1,3-dimethylnaphthalene	7.9	5.9−9.8	5.10
2-methoxynaphthalene	13	11−15	4.89
3-methylquinoline	13	9.7−17	4.89
1,5-dichloronaphthalene[a]	14	8.0−19	4.85
2-naphthol	17	15−18	4.77
2-ethylnaphthalene	19	12−26	4.72
3-methylisoquinoline	21	18−24	4.68
1,6-dimethylnaphthalene	25	17−33	4.60
quinaldine	40	34−45	4.40
1,5-dimethylnaphthalene[a]	42	29−56	4.38
2-fluoronaphthalene	49	34−64	4.31
1-chloronaphthalene	50	44−56	4.30
2,6-dimethylnaphthalene	52	33−72	4.28
2,7-dimethylnaphthalene	65	36−91	4.19
1-methylnaphthalene	110	81−150	3.96
2-methylnaphthalene	120	106−130	3.92
naphthalene	~700		3.15

[a] Used only in the external set of test compounds.

Table 2. Inhibition Potencies of Lactones and Other Compounds for CYP1A2

compd	IC_{50} (μM)	95% confidence intervals	pIC_{50}
2-(*p*-tolyl)ethylamine[a]	14	12−17	4.85
undecanoic-γ-lactone	45	34−56	4.35
4-chlorobiphenyl[a]	49	29−69	4.30
butylcyclohexane	55	45−66	4.26
γ-dodecanolactone	58	49−68	4.24
(±)-undecaonic-δ-lactone	72	53−90	4.14
2-indanone	80	51−110	4.10
γ-decanolactone	110	75−150	3.96
biphenyl	160	74−240	3.80
δ-decanolactone	230	190−270	3.64
2-chlorobiphenyl[a]	230	150−310	3.64
2-coumarone	260	170−340	3.59
4-methoxybenzaldehyde[a]	270	180−350	3.57
γ-nonanoiclactone	310	230−390	3.51
2-benzoxazolinone	370	230−510	3.43
indan	550	430−660	3.26
2,3-dihydrobenzofuran	1200	880−1500	2.92
γ-phenyl-γ-butyrolactone	2300	1600−3000	2.64
butylbenzyl	3700	2400−4900	2.43
nicotine	4100	2600−5600	2.39
4,6-dimethyl-α-pyron	4500	3300−5600	2.35
γ-heptalactone	4500	3300−5700	2.35
cotinine	5400	2400−8400	2.27
γ-caprolactone	9900	5600−14000	2.00
γ-valerolactone	15000	11000−20000	1.82
ϵ-caprolactone	>40000		>1.40
4-methoxyfuran-2(5*H*)-one	>40000		>1.40

[a] Used only in the external set of test compounds.

Tables 1 and 2 are six compounds used in the external test set. After data pretreatment, GRID/GOLPE analysis gave an r^2 value of 0.86, followed by a q^2 value of 0.73 with three components and an SDEP of 0.60. In the final model, the smart region definition (SRD) method with F.Factorial Selection was used to remove variables that did not correlate with the inhibition potency. The obtained statistics of the models are summarized in Table 3, and the plots for the training set of both models are shown in Figure 4.

Table 3. Statistics from the CoMFA and GRID/GOLPE Analyses[a]

model	q^2	r^2	S_{PRESS}/SDEP	N
CoMFA	0.69	0.87	0.67	3
GRID/GOLPE	0.79	0.90	0.52	3

[a] q^2 = the cross-validated correlation coefficient with five random groups; r^2 = correlation coefficient; S_{PRESS} (Sybyl), SDEP (GOLPE) = standard deviations for the error of predictions; N = number of PLS components.

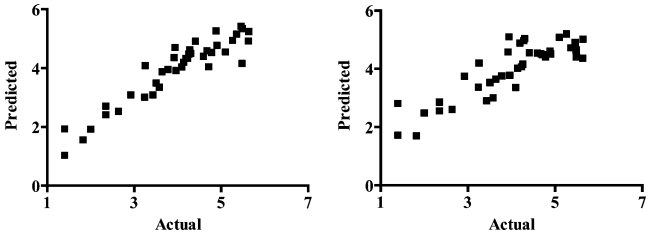

Figure 4. Plots for the training set (actual/predicted IC_{50} values) of the CoMFA model (r^2 = 0.87, left panel) and the GOLPE/GRID model (r^2 = 0.90, right panel).

The CYP1A2 CoMFA model is represented as 3D contour maps with 2,7-dimethylquinoline as the reference structure (Figure 5). The contours of the steric map are shown as green and yellow regions in which bulky groups enhance and decrease inhibition potency, respectively. Those of the electrostatic map are shown as red and blue areas in which a more negative charge enhances and decreases inhibition potency, respectively. Negative-charge-favored areas that were near a nitrogen atom and positions 6 and 8 of the quinoline ring indicate that a partial negative charge here tended to increase the inhibition potency. The broad negative-charge-disfavored area shown in blue was displayed near position 3 of the ring. The sterically favored green area was located around substitution at position 7 of quinoline in the CoMFA model.

A stereofigure of the GOLPE coefficient map (Figure 6) displays large continuous regions, where the interaction with the hydroxyl probe is favorable (cyan) or unfavorable (purple). The favorable region is around the nitrogen atom and partly above and under the aromatic ring structure. These regions of the inhibitor can act as hydrogen bond acceptors or donors. The electronic configuration of the OH probe is defined so that it interacts with the π-electron of the conjugated system like a planar aromatic ring or double bond. It makes strong hydrogen-bonding interactions, which may account for the shape of the interaction regions with the molecular structures.[16] The unfavorable regions reside in the plane of the ring and are spread all around the ring except to the region near the nitrogen atom.

The prediction power of the CoMFA model was evaluated by estimating pIC_{50} values for an external test set of compounds, including the six compounds tested in this study (Tables 1 and 2). These six compounds were chosen on the basis that they resemble in structure the ones in the training set but also contain features that differ from the training set compounds. The values for five additional compounds that are well-known

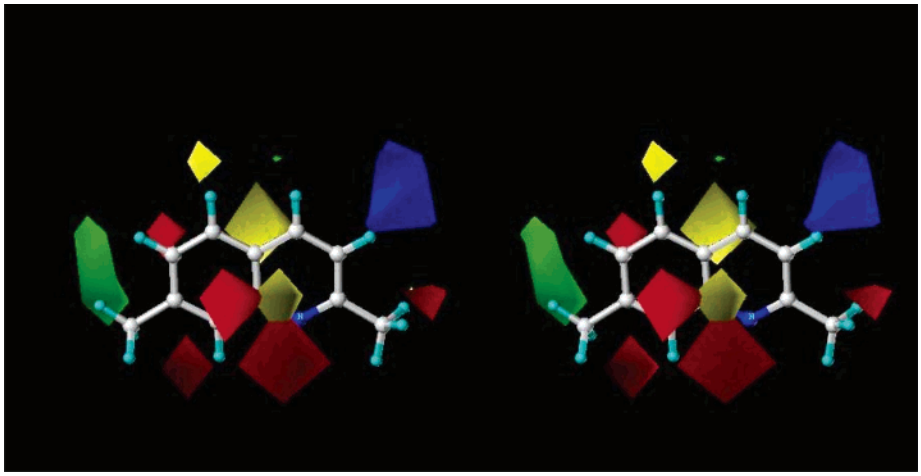

Figure 5. Stereofigure of color contour maps of CYP1A2 CoMFA. Red and green represent areas where more negative partial charge and bulkier groups increase inhibition potency, respectively. Blue and yellow represent areas where more negative partial charge and bulkier groups decrease inhibition potency, respectively. The reference structure is 2,7-dimethylquinoline.

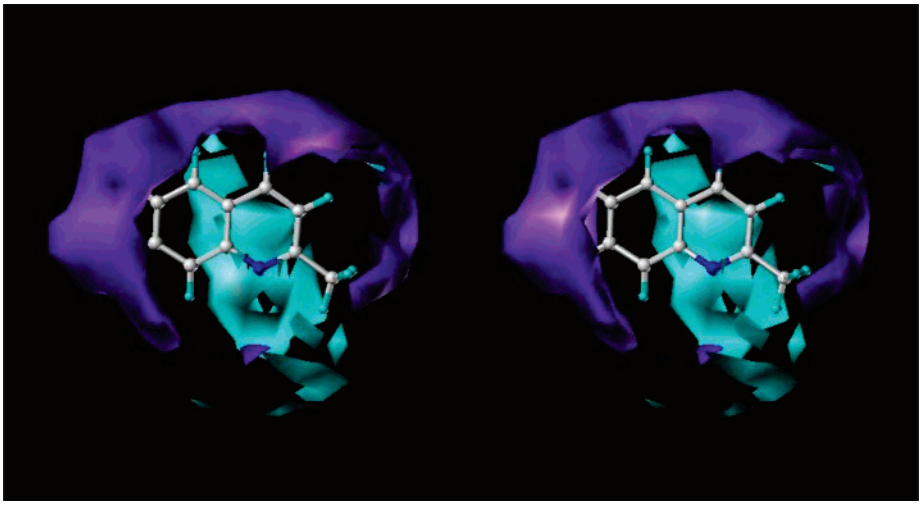

Figure 6. Stereofigure of GOLPE coefficient map with 2,7-dimethylquinoline as the reference structure. The cyan regions describe favorable interactions and the purple regions unfavorable interactions between the hydroxyl probe and the molecules.

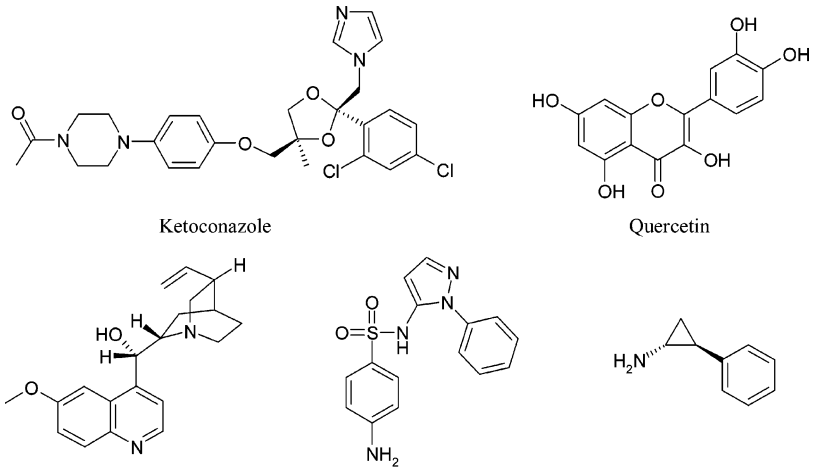

Figure 7. Structures of the external set of test compounds.

substrates and inhibitors of CYP enzymes were obtained from ref 17 (Figure 7). As summarized in Table 4, the predictions of pIC_{50} values for the external set of molecules differed by less than 0.1 log units from the actual values for biphenyls, 1,5-dichloronaphthalene, and 4-methoxybenzaldehyde. The predictions of pIC_{50} values for the other molecules were within 0.13−0.67 log unit of the actual values.

Table 4. Validation of CYP1A2 Model

inhibitor	pIC_{50}		
	experimental	predicted	residual
2-(*p*-tolyl)ethylamine	4.85	4.53	0.32
4-chlorobiphenyl	4.30	4.30	0
2-chlorobiphenyl	3.64	3.59	0.05
4-methoxybenzaldehyde	3.57	3.51	0.06
1,5-dichloronaphthalene	4.85	4.80	0.05
1,5-dimethylnaphthalene	4.38	4.80	0.42
ketoconazole[a]	4.12	4.30	0.18
quercetin[a]	5.18	5.05	0.13
quinidine[a]	4.59	3.92	0.67
sulfaphenazole[a]	>4	4.05	
tranylcypromine[a]	4.01	4.30	0.29

[a] Experimental data from ref 17.

Discussion

The main purpose of this study was to create a QSAR model to understand in greater detail the structural properties of inhibitors of the human CYP1A2 enzyme. The inhibition potency of a series of 52 chemicals was determined against the CYP1A2 enzyme. With this data set, CoMFA and GRID/GOLPE models were created that yielded novel structural information about the interaction between inhibitory molecules and the CYP1A2 active site. In addition, the developed CYP1A2 CoMFA model accurately predicted the inhibition potencies of several structurally unrelated compounds.

Some disubstituted naphthalene and quinoline derivatives were found to be potent inhibitors of CYP1A2. Quinoline derivatives had lower IC_{50} values than the corresponding naphthalene derivatives, indicating that a heterocyclic nitrogen atom increases inhibition potency. Also, hydrophobic substituents at position 1 of the naphthalene ring increase inhibition potency. Hydroxyl, halogen, and methyl substitutions of the naphthalene ring decreased the IC_{50} values. The IC_{50} values of molecules decreased as the molecular volume of lactones and the length of alkyl side chain increased.

Previously published QSAR studies on the CYP1A2 enzyme were based on a limited number of structurally diverse compounds and have not been used to predict the inhibition potency of new compounds. One of the first human CYP1A2 3D-QSAR studies was carried out on quinolone antibacterials.[9] Four pharmacophore features were suggested to be involved in the binding of quinolone-type CYP1A2 inhibitors in the active site. No correlation between lipophilicity and the inhibitory effect could be observed in this study.[9] On the basis of the experimental finding that a methyl group at position 8 of the xanthine ring is important for CYP1A2 inhibition, a subsequent theoretical model was created using a molecular electrostatic potential approach.[10] A QSAR analysis using inhibition data of 16 naturally occurring flavonoids showed that planar molecules with a small volume to surface area were the most potent inhibitors, the number of hydroxyl groups being inversely proportional to inhibition potency, and glycosylation of the free hydroxyls could reduce the inhibition potency.[11]

Two different studies docked selected substrates into the active site of homology models of the CYP1A2 protein and analyzed the binding mode of the ligand−enzyme complex in terms of molecular mechanics calculations.[12,13] Lozano et al.[13] used the COMBINE method for energy partition and adjacent 3D-QSAR analysis. Subsequently they performed a GRID/GOLPE analysis using the phenylic OH group. The combination of both methods provided useful insights into the positions of likely hydrogen bonding or placement of hydrophobic or bulky groups. A previous study suggested that CYP1A2 substrates are generally neutral or protonated molecules.[14]

The correlation between electrostatic interactions and pIC_{50} values appeared in the CoMFA maps as negative-charge-favored areas that are near the nitrogen atom of the quinoline ring. Also, electronegative substituents at position 1 of the naphthalene ring are important for inhibition. This explains the finding that 1,4-dichloronaphthalene and 1-naphthol are quite potent inhibitors compared with the naphthalenes with halogen or other electronegative substituent at position 2. In addition, there is an attractive interaction between the hydroxyl probe and an inhibitor favorable area located around position 1 of the quinoline ring near the nitrogen atom. The hydroxyl probe is capable of donating and accepting one hydrogen bond with a hydrogen acceptor or donor atom or with the π-system of the aromatic ring. GRID/GOLPE maps can describe interactions between nitrogen and the hydroxyl group or dipole-induced dipole interactions between the aromatic ring and the probe.[16] The nitrogen atom can act as a hydrogen-bonding acceptor atom, which indicates that hydrogen bonding is an important interaction between quinoline-type inhibitors and the CYP1A2 enzyme.

Most of the CYP1A2 substrates are hydrophobic with high log *P* values, suggesting that hydrophobic interactions play an important role in binding to CYP1A2. The created CoMFA model confirms this because the CoMFA model shows that alkyl substitutions at position 7 increase the inhibitory potency. The alkyl side chain of lactones can interact with hydrophobic amino acids in the CYP1A2 protein. A large steric-favored region is located near the 7-position in the CoMFA map. Also, substitution of naphthalene with hydrophobic substituents such as halogen or methyl groups increases the inhibition potency. These data suggest that the binding pocket of the CYP1A2 enzyme is composed of mostly hydrophobic and aromatic amino acids, with polar amino acids for hydrogen bonding being present near the heme center.[18] In addition to the use of steric and electrostatic fields, a CoMFA model was created using log *P* values as an additional variable. This did not improve in the model.

The created CoMFA model predicted very well the inhibitory potencies of the test set of compounds. The best predictions were obtained for biphenyls and 1,5-dichloronaphthalene, with predicted pIC_{50} values being within 0.05 log units of the actual values. The model also predicted well the CYP1A2 pIC_{50} values of several well-known inhibitors of other cytochrome P450 forms, ketoconazole (CYP3A4), tranylcypromine (CYP2A6), quinidine (CYP2D6), quercetin (CYP2C8), and sulfaphenazole (CYP2C9).[7] This is remarkable because the structures of these compounds differ considerably from the ones used in the training set.

The current CoMFA model takes into account both steric and electrostatic interactions. The CoMFA approach described in this report represents a robust method to screen for inhibitory properties of compounds

toward CYP1A2. A similar approach will be applicable to other xenobiotic metabolizing cytochrome P450 compounds as well. We have shown earlier that CoMFA modeling can predict reasonably well the actual inhibition characteristics of lactones and naphthalenes toward the human CYP2A6 and mouse CYP2A5 enzymes and that naphthalene is metabolized by these CYP forms.[19,20] A CoMFA method similar to the one described here has been used for modeling the CYP2A6 enzyme.[21] In the present CYP1A2 QSAR study, the GRID/GOLPE analysis was also applied, which improved the precision of the model through exclusion of variables that were not significant.

The model presented here is clearly superior to previously published QSAR models of CYP1A2. The current training set is large and contains structurally diverse compounds. All biological data used in the training set are generated with internally fully consistent methods. The model is reasonably predictive even for compounds that differ in structure from the ones in the training set. Using the hydroxyl probe yielded information about the importance of dipole-induced dipole interaction in the active site of CYP1A2. The GRID/GOLPE analysis gave insight into the shape of the interaction regions. The presented CoMFA and GRID/GOLPE models are in agreement with previous studies concerning areas of H-bonds and electrostatic field.[9−13] However, from the statistical analysis of a large training set with structurally diverse compounds, the present model is more general and predictive than the previous ones. In particular, the spatial orientation in the regions where H-bonds are likely to occur and the regions where bulky groups enhance the inhibitory potential could be determined in both a qualitative and a quantitative way.

There are two major reasons for studying inhibitory potencies of drug candidates and other xenobiotics. First, potent inhibition by a drug candidate gives an early warning about potential drug−drug interactions during its clinical use. Second, evidence of inhibition capabilities suggests that the compound may be a substrate for the cytochrome P450 studied. This applies especially to competitive inhibitors. Because competitive inhibitors are usually also substrates of cytochrome P450, screening of inhibitory properties serves as a good starting point for substrate specificity studies for any chemical compound. Inhibitor orientation in the CoMFA model provides clues on how it is coordinated toward the cytochrome P450 heme iron if the oxidation pattern of at least one molecule in the training set is known. Thus, a CoMFA model based on inhibition data can represent a starting point to the much more complex task of predicting the metabolism of novel compounds.

A recent report has described a computational filter for prediction of inhibitory properties of compounds toward CYP2D6 and CYP3A4 enzymes. The filter, based on training sets of more than 1700 molecules, yielded a statistically significant rank ordering of test set molecules.[22] There is now considerable interest in the development of computational methods to assess cytochrome P450 mediated metabolic properties of drug candidates and other xenobiotics. Initial attempts are being made to create databases combining different approaches for the prediction of metabolism.[23]

In the future these kinds of computer models may become very efficient for predicting the structural requirements of inhibitors of cytochrome P450. In particular, the combination of QSAR and protein models offers a potentially very powerful approach for predicting cytochrome P450 mediated metabolism.

Experimental Section

Chemicals. γ-Heptalactone, ϵ-caprolactone, γ-decanolactone, γ-dodecanolactone, γ-caprolactone, 4,6-dimethyl-α-pyrone, 1,3-dimethylnaphthalene, and 1,4-dimethylnaphthalene were purchased from Sigma-Aldrich (St. Louis, MO). Undecanoic-γ-lactone, γ-valerolactone, δ-decanolactone, γ-phenyl-γ-butyrolactone, (±)-undecaonic-δ-lactone, γ-nonanoic-lactone, 2,3-dihydrobenzofuran, 4-methoxyfuran-2(5*H*)-one, 2-benzoxazolinone, butylbenzyl, 2-indanone, 2-coumarone, indan, butylcyclohexane, 2,7-dimethylnaphthalene, 2-methoxynaphthalene, 2-(*p*-tolyl)ethylamine, 1-methylnaphthalene, quinaldine, 2-ethylnaphthalene, 1,5-dimethylnaphthalene, 2,6-dimethylquinoline, 2-methylnaphthalene, 1,6-dimethylnaphthalene, 3-methylisoquinoline, 2,6-dimethylnaphthalene, 2,7-dimethylquinoline, 3-methylquinoline, 1,2-dimethylnaphthalene, 2,4-dimethylquinoline, 2-naphthol, and naphthalene were purchased from Aldrich-Chemie GmbH & Co. (Heidenheim, Germany). Biphenyl and 1,7-dimethylnaphthalene were purchased from Fluka Chemie AG (Buchs, Switzerland). 2-Chlorobiphenyl, 4-chlorobiphenyl, 1,4-dichloronaphthalene, 1,5-dichloronaphthalene, and 1-chloronaphthalene were from Promochem (Boras, Sweden). 4-Methoxybenzaldehyde, 1-naphthol, nicotine, cotinine, and 7-ethoxyresorufin were from Sigma Chemical Co. (St. Louis, MO). 2-Fluoronaphthalene was from Supelco (St. Louis, MO). NADP was from Roche Diagnostic GmbH (Mannheim, Germany). The purity of all compounds used was higher than 95% according to the manufacturers.

Biological Material. Human liver samples used in this study were obtained from the University Hospital of Oulu as surplus from kidney transplantation donors. The collection of surplus tissue was approved by the Ethics Committee of the Medical Faculty of the University of Oulu, Oulu, Finland. The livers were transferred to ice immediately after surgical excision, cut into pieces, snap-frozen in liquid nitrogen, and stored at −80 °C until the microsomes were prepared by standard differential ultracentrifugation. A weight-balanced microsomal pool of seven liver microsomal preparations that have been extensively characterized for primary metabolic screening was employed.

Baculovirus-insect cell expressed human CYP1A2 was purchased from Gentest Corp. (Woburn, MA).

Biochemical Assays. The 7-ethoxyresorufin O-dealkylation assay is based on the detection of fluorescence emitted by resorufin.[24] The assay was adapted to the 96-well plate format. In each well, a 150 μL incubation volume contained 100 mM Tris-HCl buffer (pH 7.4), 4.2 mM $MgCl_2$, 1 μM 7-ethoxyresorufin, 0.5 pmol of cDNA expressed CYP1A2, 0−40 mM inhibitor, and a NADPH-generating system.[24] All inhibitors were dissolved in ethanol, and the final concentration of ethanol was 2% in all incubations. The reaction was initiated by adding the NADPH-regenerating system after a 10 min preincubation at 37°C, and after a 20 min incubation, the reaction was terminated by the addition of 110 μL of 80% acetonitrile/20% 0.5 M Tris base. The formed fluorescence was measured with a Victor^2 plate counter (Perkin-Elmer Life Sciences Wallac, Turku, Finland) at 570 nm excitation and 616 nm emission. The linearity of the reaction with respect to incubation time and protein concentration was determined. Several control incubations were carried out to determine the effect of quenching by the inhibitors and other interfering factors. Each inhibitor was prescreened using pooled human liver microsomes at inhibitor concentrations ranging from 0.1 to 40 000 μM. The actual IC_{50} values were determined using expressed human CYP1A2 enzyme and seven inhibitor concentrations. The IC_{50} values were calculated using nonlinear

regression analysis with Prism 4.0 software (San Diego, CA) from the results of two separate experiments.

Because the purpose of this study was to create a model for CYP1A2 enzyme inhibition, IC_{50} values (measuring relative inhibition potency) rather than the absolute K_i values were determined. This is justified because all measurements were made under standardized conditions, and the results are thus fully comparable with each other.

CoMFA and GRID/GOLPE Models. The construction of the molecules, superimposition, and CoMFA modeling were performed using the Sybyl 6.9 (Tripos Associates Inc., St. Louis, MO) molecular modeling software. The biological data was transformed to pIC_{50} ($-\log IC_{50}$) values.

Atomic point charges were calculated using the MMFF94 method. Standard CoMFA analysis included steric and electrostatic fields that were calculated using the sp^3 carbon probe atom with a +1 charge and a 2 Å grid spacing. The standard derivation threshold for exclusion of columns from the partial least squares (PLS) analysis was set at 2 kcal/mol. The PLS method with five random group cross-validations was used for statistical analyses, and this calculation was repeated 20 times to verify the stability of the obtained q^2 values. The optimum number of components for the nonvalidated analyses was chosen using the lowest S_{PRESS} value and the highest q^2 value. The predictive capacity of the generated model was tested using an external set of compounds (Table 6).

In addition to the standard CoMFA model, another model was created using the GRID/GOLPE method. GRID fields were created using a phenolic hydroxyl probe with 1 Å grid spacing, and the positive cutoff was set to 5 kcal/mol. The phenolic hydroxyl probe was chosen because it represents a hydrogen bond donor or acceptor that was found to be suitable for examining aromatic systems. GRID fields of the molecules were analyzed with GOLPE.[25,26]

Initially the GRID/GOLPE analysis included several variables that did not describe interactions between inhibitory molecules and the GOLPE hydroxyl probes. Therefore, the SRD and the F.Factorial Selection procedures were used to reduce the number of variables in the final GOLPE model. Data pretreatment was done using the zeroing option correction. To diminish the amount of noise in the data, positive values smaller than 0.10 and negative values greater than −0.01 were zeroed. The SRD analysis was performed to select important variables for the interaction using a maximum dimensionality of 5 with a critical distance cutoff value of 1 Å and with a collapsing distance cutoff value of 2 Å. The F.Factorial Selection procedure was used with a maximum dimensionality of 2, and the Random Groups method was used with five groups to separate a variable that significantly improves predictability. The final model was validated by using PLS cross-validation with five random groups.

Acknowledgment. We thank Hannele Jaatinen for expert technical assistance, Toni Rönkkö, M.Sc., and Outi Salo, M.Sc., for advice on QSAR methods, and Dr. Ewen MacDonald for comments on the manuscript. Human liver microsomes and some of the chemicals used were provided by Dr. Miia Turpeinen and Prof. Olavi Pelkonen (Department of Pharmacology and Toxicology, University of Oulu). This work was supported by grants from the National Technology Agency of Finland, TEKES (Projects 40187/04 and 40002/04).

References

(1) Eaton, D. L.; Gallagher, E. P.; Bammler, T. K.; Kunze, K. L. Role of cytochrome P4501A2 in chemical carcinogenesis: Implications for human variability in expression and enzyme activity. *Pharmacogenetics* **1995**, *5*, 259−274.

(2) Guengerich, F.; Parikh, A.; Turesky, R.; Josephy, P. Interindividual differences in the metabolism of environmental toxicants: Cytochrome P450 1A2 as a prototype. *Mutat. Res.* **1999**, *428*, 115−124.

(3) Butler, M. A.; Iwasaki, M.; Guengerich, F. P.; Kadlubar, F. F. Human cytochrome P-450PA (P-450IA2), the phenacetin *O*-deethylase, is primarily responsible for the hepatic 3-demethylation of caffeine and N-oxidation of carcinogenic arylamines. *Proc. Natl. Acad. Sci. U.S.A.* **1989**, *86*, 7696−7700.

(4) Robson, R. A.; Matthews, A. P.; Miners, J. O.; McManus, M. E.; Meyer, U. A.; Hall, P. M.; Birkett, D. J. Characterisation of theophylline metabolism in human liver microsomes. *Br. J. Clin. Pharmacol.* **1987**, *24*, 293−300.

(5) Sesardic, D.; Boobis, A. R.; Murray, B. P.; Murray, S.; Segura, J.; de la Torre, R.; Davies, D. S. Furafylline is a potent and selective inhibitor of cytochrome P450IA2 in man. *Br. J. Clin. Pharmacol.* **1990**, *29*, 651−663.

(6) Brosen, K.; Skjelbo, E.; Rasmussen, B. B.; Poulsen, H. E.; Loft, S. Fluvoxamine is a potent inhibitor of cytochrome P4501A2. *Biochem. Pharmacol.* **1993**, *45*, 1211−1214.

(7) Pelkonen, O.; Maenpaa, J.; Taavitsainen, P.; Rautio, A.; Raunio, H. Inhibition and induction of human cytochrome P450 (CYP) enzymes. *Xenobiotica* **1998**, *28*, 1203−1253.

(8) Ekins, S.; de Groot, M. J.; Jones, J. P. Pharmacophore and three-dimensional quantitative structure activity relationship methods for modeling cytochrome p450 active sites. *Drug Metab. Dispos.* **2001**, *29*, 936−944.

(9) Fuhr, U.; Strobl, G.; Manaut, F.; Anders, E. M.; Sorgel, F.; Lopez-de-Brinas, E.; Chu, D. T.; Pernet, A. G.; Mahr, G.; Sanz, F. Quinolone antibacterial agents: Relationship between structure and in vitro inhibition of the human cytochrome P450 isoform CYP1A2. *Mol. Pharmacol.* **1993**, *43*, 191−199.

(10) Sanz, F.; Lopez-de-Brinas, E.; Rodriques, J.; Manaut, F. Theoretical study on the metabolism of caffeine by cytochrome P-450 1A2 and its inhibition. *Quant. Struct.−Act. Relat.* **1994**, *13*, 281−284.

(11) Lee, H.; Yeom, H.; Kim, Y. G.; Yoon, C. N.; Jin, C.; Choi, J. S.; Kim, B. R.; Kim, D. H. Structure-related inhibition of human hepatic caffeine N3-demethylation by naturally occurring flavonoids. *Biochem. Pharmacol.* **1998**, *55*, 1369−1375.

(12) De Rienzo, F.; Fanelli, F.; Menziani, M. C.; De Benedetti, P. G. Theoretical investigation of substrate specificity for cytochromes P450 IA2, P450 IID6 and P450 IIIA4. *J. Comput.-Aided Mol. Des.* **2000**, *14*, 93−116.

(13) Lozano, J. J.; Pastor, M.; Cruciani, G.; Gaedt, K.; Centeno, N. B.; Gago, F.; Sanz, F. 3D-QSAR methods on the basis of ligand−receptor complexes. Application of COMBINE and GRID/GOLPE methodologies to a series of CYP1A2 ligands. *J. Comput.-Aided Mol. Des.* **2000**, *14*, 341−353.

(14) Lewis, D. F. V. On the recognition of mammalian microsomal cytochrome P450 substrates and their characteristics. *Biochem. Pharmacol.* **2000**, *60*, 293−306.

(15) Moon, T.; Chi, M. H.; Kim, D.; Yoon, C. N.; Choi, Y. Quantitative structure−activity relationship (QSAR) study of flavonoid derivatives for inhibition of cytochrome P450 1A2. *Quant. Struct.−Act. Relat.* **2000**, *19*, 257−263.

(16) Pastor, M.; Cruciani, G.; Clementi, S. Smart region definition: A new way to improve the predictive ability and interpretability of three-dimensional quantitative structure−activity relationships. *J. Med. Chem.* **1997**, *40*, 1455−1464.

(17) Turpeinen, M.; Uusitalo, J.; Jalonen, J.; Pelkonen, O. Multiple P450 substrates in a single run: rapid and comprehensive in vitro interaction assay. *Eur. J. Pharm. Sci.* **2005**, *24*, 123−132

(18) Dai, R.; Pincus, M. R.; Friedman, F. K. Molecular modeling of mammalian cytochrome P450s. *Cell. Mol. Life Sci.* **2000**, *57*, 487−499.

(19) Juvonen, R. O.; Gynther, J.; Pasanen, M.; Alhava, E.; Poso, A. Pronounced differences in inhibition potency of lactone and nonlactone compounds for mouse and human coumarin 7-hydroxylases (CYP2A5 and CYP2A6). *Xenobiotica* **2000**, *30*, 81−92.

(20) Asikainen, A.; Tarhanen, J.; Poso, A.; Pasanen, M.; Alhava, E.; Juvonen, R. O. Predictive value of comparative molecular field analysis modelling of naphthalene inhibition of human CYP2A6 and mouse CYP2A5 enzymes. *Toxicol. in Vitro* **2003**, *17*, 449−455.

(21) Rahnasto, M.; Raunio, H.; Poso, A.; Wittekindt, C.; Juvonen, R. O. Quantitative structure−activity relationship analysis of inhibitors of the nicotine metabolizing CYP2A6 enzyme. *J. Med. Chem.* **2005**, *48*, 440−449.

(22) Ekins, S.; Berbaum, J.; Harrison, R. K. Generation and validation of rapid computational filters for cyp2d6 and cyp3a4. *Drug Metab. Dispos.* **2003**, *31*, 1077−1080.

(23) Erhardt, P. W. A human drug metabolism database: Potential roles in the quantitative predictions of drug metabolism and metabolism-related drug−drug interactions. *Curr. Drug Metab.* **2003**, *4*, 411−422.

(24) Burke, M. D.; Thompson, S.; Elcombe, C. R.; Halpert, J.; Haaparanta, T.; Mayer, R. T. Ethoxy-, pentoxy- and benzyloxyphenoxazones and homologues: A series of substrates to distinguish between different induced cytochromes P-450. *Biochem. Pharmacol.* **1985**, *34*, 3337−3345.

(25) Wade, R. C.; Clark, K. J.; Goodford, P. J. Further development of hydrogen bond functions for use in determining energetically favorable binding sites on molecules of known structure. 1. Ligand probe groups with the ability to form two hydrogen bonds. *J. Med. Chem.* **1993**, *36*, 140−147.

(26) Baroni, M.; Constantino, G.; Cruciani, G.; Riganelli, D.; Valigi, R.; Clementi, S. Generating optimal linear PLS estimations (GOLPE): An advanced chemometric tool for handling 3D-QSAR problems. *Quant. Struct.−Act. Relat.* **1993**, *12*, 9−20.

JM0489713